2013 IEEE/RSJ International Conference on
Intelligent Robots and Systems (IROS)
November 3-7, 2013. Tokyo, Japan

Development of an Antagonistic Bionic Joint Controller for a Musculoskeletal Quadruped*

Xin Wang, *Student Member, IEEE*, Mantian Li, Wei Guo, Pengfei Wang and Lining Sun

Abstract— **In this paper, a joint control algorism was proposed to implement on our musculoskeletal robot. The joints are all actuated by pneumatic muscles and have antagonistic structure. In order to gain a better performance, we first modeled the pneumatic muscle, and then considering the dynamics two control method was discussed and compared. As a tradeoff of rapidity and accuracy, the combined joint control algorism was implemented on the robot system. The algorism could tune the stiffness of the joint automatically to fit the compliance need for joint control. The experiments on our robot showed that the joint control algorism could operate the robot with a fast and accurate response. There is nearly not lagging behind, and with a small overshot during the step testing, and a complex leg's trajectory was also achieved through our joint controller.**

I. Introduction

In the last years, a lot of research works has shown the benefits of using biological principles for robot design, especially incorporated into the mechanical and controller design. In order to have a compliant joint character, many researchers focused on the artificial muscles. Tondu and et al ever set a robot-arm actuated by McKibben muscles which behaves soft and well adapted to human contact or fragile environment [1]. This specific property constitutes the foundation of the actuator natural compliance.

For the biological inspired robotics, it is obviously that artificial muscles as actuators are the nearest models of the biological actuator [2]. In University of Tokyo, their research group has designed a series musculoskeletal humanoid robot, such as Kotaro [3], Kojiro [4], Kenzoh [5] and the newest one Kenshiro which has detailed human imitating points over whole-body [6]. For the quadruped robot, PANTER is a prototype for fast running with pneumatic muscles [7]. The ideal of PANTER is to have a closer look at the principles used in natured and to evaluate where and how they can be adapted to robotics. Kurt S. Aschenbeck and et al also built a quadruped robot driven by Festo pneumatic muscles [8].

* This work is supported by National Hi-tech Research and Development Program of China (863 Program, Grant No. 2011AA0403837002), National Natural Science Foundation of China (No. 61005076, No. 61175107).

Xin Wang is currently a PhD candidate in State Key Laboratory of Robotics and System, Harbin Institute of Technology, 150001, China (phone: 86-451-86402217; E-mail: xinwanghit07s@gmail.com).

Mantian Li, Wei Guo and Lining Sun is in State Key Laboratory of Robotics and System, Harbin Institute of Technology, 150001, China (E-mail: {limt, wguo01, lnsun}@hit.edu.cn).

Pengfei Wang is currently an associate professor in State Key Laboratory of Robotics and System, Harbin Institute of Technology, 150001, China (E-mail: wangpengfei1007@163.com).

The chosen of pneumatic muscles to actuate the robot is due to their light-weight, naturally compliant, high force-weight ratio and properties similar to biological muscle. Colbrunn and et al proposed a control method to have a tunable stiffness properties at each joint [9]. In order to have compliance joint, Bram Vanderborght and et al proposed a strategy to combine active trajectory tracking for bipedal robot "Lucy" with exploiting the natural dynamics by simultaneously controlling the torque and stiffness of pneumatic muscles [10]. Due to the pneumatic muscles performing as a complex behavior, researchers are interesting in modeling accurately and controlling muscles based on the model robustly [11], even some researchers imitate nervous system to active pneumatic artificial muscles systems [12].

In this paper, an antagonistic joint control strategy is proposed to combine the closed loop position tracking by simultaneously the open loop force controlling based on a pneumatic muscle model. The controller is developed for our "cheetah" robot, as shown in Fig.1, which is actuated by pneumatic artificial muscles toward ultra high speed. The robot consists of a rigid torso with hind- and fore-limbs which share the same basic concept of a "z" type construction. There are three active controlled articulations (hip, knee, ankle for hindlimb, and STC, shoulder, elbow for forelimb) and one passive joint (MTP and MCP) for each leg [13].

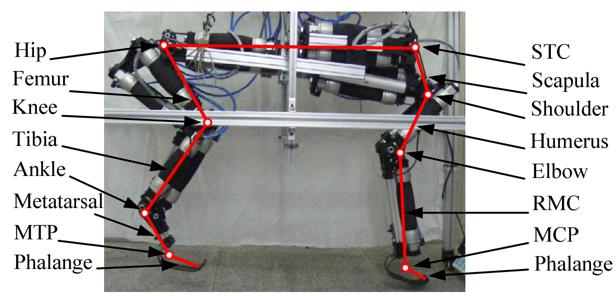

Figure 1. The cheetah robot system.

All of the active controlled articulations are actuated by FESTO pneumatic artificial muscles. These muscles are fed with compressed air through proportional pressure valves. The major problem is that the muscle can only develop tractive force, thus it need for two antagonistic muscles for each joint. Additionally, the robot demands a fast and accurate response with tunable stiffness [14], which brings us more troubles on joint controller design. Thus we first modeled the pneumatic muscle in the section II. Then, we discussed the properties of two types of joint control methods, in section III. Finally, a combining control strategy was proposed as a tradeoff between various factors. The quality of the control strategy was verified by implementing on the cheetah robot system in section IV.

II. MODEL OF ANTAGONISTIC JOINT

A. Pendulum Model

For legged robot, pendulum model is the basic dynamic model, because the behaviors of the swing leg are just like a pendulum swinging, and the stance leg like an inverted pendulum. In each joint of our robot, two pneumatic muscles are arranged antagonistically to actuate one joint swinging. As shown in Fig.2, a regular pendulum model was chosen to describe the behaviors of each joint and segment as a general model.

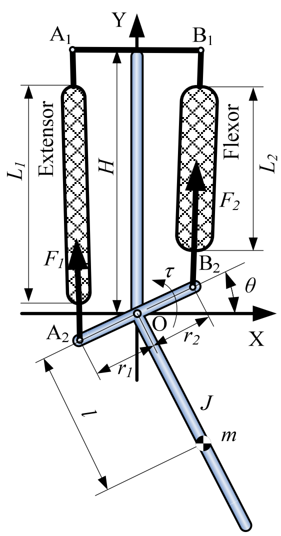

Figure 2. Antagonistic pneumatic muscles actuated joint model.

The dynamic physical properties of the joint are

$$(J+ml^2)\ddot{\theta}+c\cdot\dot{\theta}+mgl\cdot\cos\theta=\tau\,, \tag{1}$$

$$L_i=\sqrt{(H\pm r_i\cdot\sin\theta)^2+(r_i-r_i\cdot\cos\theta)^2}-L_i^c=L_{ni}\cdot(1-\varepsilon)\quad(i=1,2)\,, \tag{2}$$

$$\begin{aligned}\tau(F_1,F_2,\theta)=&\ F_1\cdot r_1\cdot\cos[\theta-\arctan\left(\frac{r_1-r_1\cdot\cos\theta}{H+r_1\cdot\sin\theta}\right)]\\&-F_2\cdot r_2\cdot\cos[\theta+\arctan\left(\frac{r_2-r_2\cdot\cos\theta}{H-r_2\cdot\sin\theta}\right)]-mgl\cdot\sin\theta\end{aligned}\,, \tag{3}$$

where, J and m are the inertia and the mass of the segment; τ is the articulated load moment; L_i is the length of the pneumatic muscle; H is the length of the 'bone'; θ is the angle of the joint; L^c_i is the length of the accessories and connectors which is unchanged during stretching; L_{ni} is the normal length of the muscle; ε is the contraction rate of the muscle.

B. Pneumatic Muscle Model

To use the pneumatic muscles as a tunable stiffness system or a torque controllable actuator it is necessary to have an accurate model which could describe the dynamic process. The Chou model is a classical model which is based on geometrical relationships [15], and many researchers did some modifications on dynamic properties [2] and hysteresis [16]. But these models are all maximally correlated to the muscles geometric parameters. There is only a force and displacement diagram for pneumatic muscles of the FESTO Company, as shown in Fig.3. The data of muscle's force/pressure/displacement for the model approximating can be got from the diagram in Fig.3. Thus, Tondu-Lopez model [17, 18] was chosen as the least squares approximation F^* for contracting force of the muscle F,

$$F^*(p,\varepsilon)=f_1(p)-100\cdot f_2(p)\varepsilon+f_3(p)e^{-40\varepsilon}\,, \tag{4}$$

where, p is the inner pressure of the muscle; $f\,(p)$ is the parameter function group of p, which is to be determined. Then, the work we should do is to find a $F^*(p,\varepsilon)\in\Phi$, where Φ is a family of square integrable function, to make

$$\left\|F(p,\varepsilon)-F^*(p,\varepsilon)\right\|=\min_{\tilde{F}\in\Phi}\left\|F(p,\varepsilon)-\tilde{F}(p,\varepsilon)\right\|\,. \tag{5}$$

We assume that the variables p and ε are uncorrelated, thus the approximating can be operated independently. First we take f_1, f_2, f_3 as the undetermined coefficients and ε as the variables, to find the approximation functions $F^{*(p)}$ under different pressures $p=[0, 1, 2, 3, 4, 5, 6]$ independently. Thus, we can get a series of $F^{*(p)}$,

$$F^{*(p)}(\varepsilon)=f_1^{(p)}-100\cdot f_2^{(p)}\varepsilon+f_3^{(p)}e^{-40\varepsilon}\,. \tag{6}$$

Secondly, we take $f_i(p)$ as a function of p to find the approximation functions $f_i^*(p)$, where the vectors $(p, f_i^{(p)})$ are the points on $f_i(p)$, $i=1,2,3$. The polynomial fitting was used to approximate $f_i(p)$, and the fitting results are

$$\begin{cases}f_1^*(p)=972p-352.5\\ f_2^*(p)=30.17p+4.195\\ f_3^*(p)=14.05p^2-60.77p+488.3\end{cases}\,. \tag{7}$$

Take (7) into (4), we can get the least squares approximation

$$\begin{aligned}F^*(p,\varepsilon)=&\,(972p-352.5)-(3017p+419.5)\varepsilon\\&+(14.05p^2-60.77p+488.3)\cdot e^{-40\varepsilon}\end{aligned}\,. \tag{8}$$

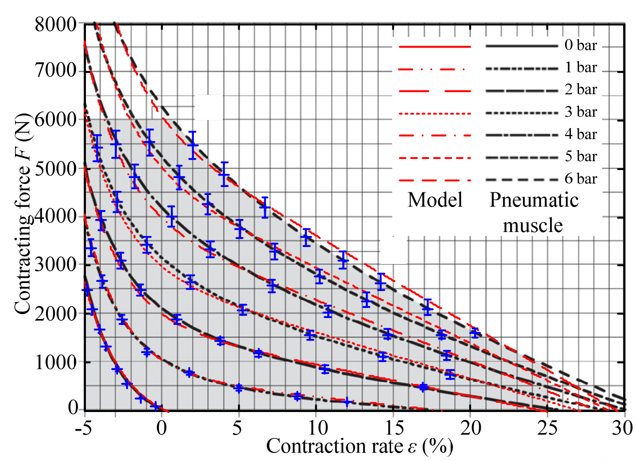

Figure 3. The comparision between muscle model and FESTO diagram. The blue bar pressents the 95% confidence bounds.

During the approximating, the adjusted R-square for any time of fitting is higher than 0.99. The comparison of F^* and F in Fig.3 shows that the whole model are all within the 95% confidence bounds, which is sufficient for control purposes.

C. The Properties of Antagonistic Joint

■ The muscle model described the relationship of force, pressure, and displacement. The displacement of muscle, equally the contraction rate ε, is related to the joint angle θ, which can be sensed by absolute encoder. That means we can control the muscle's output force using the muscle model through controlling the muscle's inner air pressure. So without additional force or torque sensors, the pneumatic muscles can be controlled in an open loop under the muscle model and the joint dynamics. Moreover, it also can be used in a closed force control loop, while the force feedback is realized with muscle model by calculating (8). This property of the pneumatic muscles brings benefits and flexibility on the constructing of the joint control architecture.

■ A notable characteristic of mammals' joint is compliance, and adaptable compliance is important for mammal walking and running. Due to the gas compressibility the pneumatic muscle is compliant. Thus, the joint compliance for our robot can be generated directly by the use of the antagonistic pneumatic muscles. The joint stiffness, the inverse of compliance, can be obtained by taking a derivative of the torque with respect to joint angle. Taking (3), the nonlinear formulae causing by joint geometric construction can be eliminated due to the little influence. Thus, joint stiffness is

$$k = \frac{d\tau}{d\theta} \approx r_1 \frac{dF_1}{d\theta} - r_2 \frac{dF_2}{d\theta} = -\frac{r_1^2}{L_{n1}} \cdot \frac{dF_1}{d\varepsilon_1} - \frac{r_2^2}{L_{n2}} \cdot \frac{dF_2}{d\varepsilon_2}, \quad (9)$$

where, $dF/d\varepsilon$ could represent the stiffness of a muscle. By differentiating (8), we can get $dF/d\varepsilon$, and because of ε the value is negative,

$$\begin{aligned} \frac{dF}{d\varepsilon} &= -562e^{-40\varepsilon} \cdot p^2 - (3017 - 2430.8e^{-40\varepsilon})p \\ &\quad -(419.5 + 19532e^{-40\varepsilon}) \end{aligned}. \quad (10)$$

Taking (10) into (9), we can obtain k. For a fixed position, the stiffness of muscle is a parabolic profile about p with the symmetric axis on the negative plane. Thus, at any joint position, the stiffness of muscles is monotone decreasing, while the stiffness of joint is monotone increasing about pressure. That means via controlling the pressure we can also get a tunable joint stiffness.

■ The pneumatic muscles are working in antagonism with initial contraction rate 10% for each joint of our robot. The muscles are activated as the agonist is inflated for flexion and the antagonist is deflated for extension. As shown in Fig.4, if the external force of the joint is constant and the starting position of the joint is A, the agonist and antagonist will choose different paths to make the joint swing from one angle to another angle. Although the muscles are arranged symmetrically, the processes of flexion and extension are asymmetric due to the nonlinear of the muscles. As shown in Fig.4, the agonist flexed along the path AB by inflating Δp_2, while the antagonist extended along the path AC by deflating Δp_1. The values of Δp_1 and Δp_2 are obviously not equal. Moreover, the properties, such as slope and gradient, of the paths AB and AC are also different. So, for the control system, it is better to use different parameters for the control of the agonist and the antagonist.

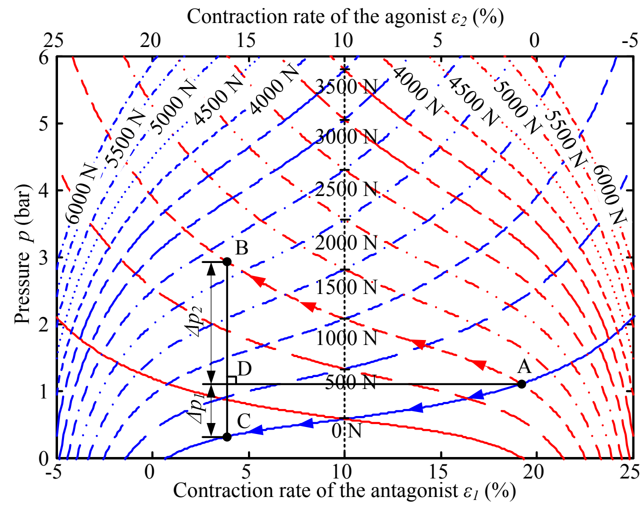

Figure 4. The contour map of antagonistic muscles force. The red line presents the agonist and the blue line presents the antagonist.

III. Joint Control

A. The Basic Position Control Method (BPC)

A natural ideal of controlling the antagonistic joint is through controlling the lengths of two muscles. The closed loop control is necessary to perform accurate movements in a feasible way for our robot. As discussed above, the agonist and the antagonist are controlled through two PID controllers independently, as shown in Fig.5. Through calculating the joint geometric equation (2), the desired muscle length L_i^d and the current muscle length L_i can be obtained to compute the error L_i^e for PID controller. The parameters of PID controller are different for the antagonist system and the agonist system, and were chosen by trial and error. The parameters for the antagonist muscle are smaller than the agonist ones, which could produce the same effect as the example shown in Fig.4. It caused the variation of the antagonist pressure smaller, slower, and gentler than the agonist one.

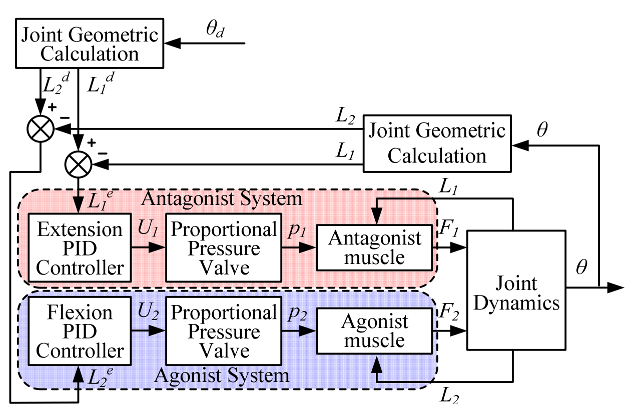

Figure 5. The basic position control diagram.

It is notable that for the antagonistic system the functions of the muscles are not invariable. Whether a muscle is the antagonist or agonist, it is decided by the desired and the current angles. As shown in Fig.6 (a), when the desired angle is beyond the current angle, the left muscle is agonist. Contrarily as in Fig.6 (b), when the current angle is beyond the desired angle, the left one becomes antagonist, although these two states of the joint are looking similar. The control strategy of muscles would be changing simultaneously while the functions of the muscles exchanged.

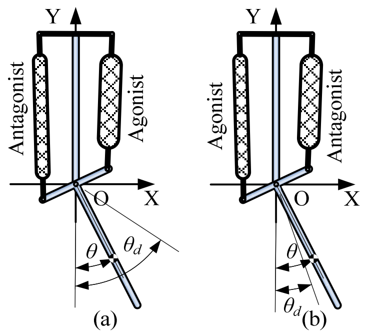

Figure 6. The variation of the muscles.function.

B. The Model Based Position Control Method (MBPC)

Mammals' joints are unexceptionally antagonistic type. But during the joint movements, only the agonist muscle is activated by neuron. The antagonist muscle is relaxed during joint swinging, which we considered it as a force servo system. As section II C discussed, we can obtain an inaccurate muscle force control based on the muscle model. Thus, a model based position control method was proposed as shown in Fig.7, which we thought more bionic. Unlike the basic position control method, the antagonist muscle is controlled under an open loop force control. Given the desired force F_1^d and the contraction rate ε_1 which is a smooth curve generated through comparing the desired length L_1^d and the current length L_1, the muscle model could calculate the need of the pressure to make the muscle force F_1 approximate equal to F_1^d. The F_1^d can be set very small even zero, which could reduce the antagonistic forces and make the joint swinging unhindered. The agonist muscle is under the regular closed loop position control, which is to guarantee the precision of the joint position and the PID controller could absorb the perturbation due to the inaccurate of the muscle model.

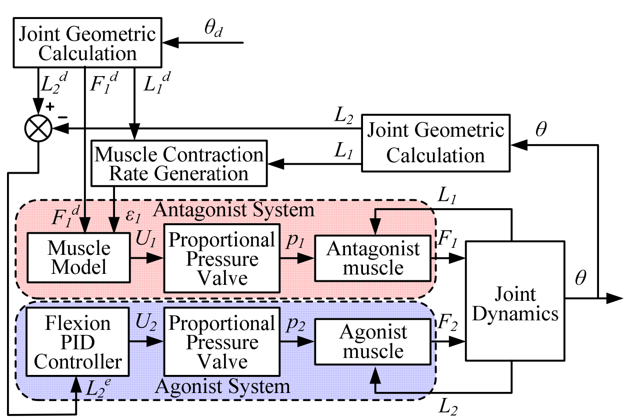

Figure 7. The model based position control diagram.

C. Comparison and Discussion

■ Rapidity

The properties of the controller was tested through an angle following. The desired angles were varied between 15° to -15° with slopes ±100°/s. The results of two control method were shown in Fig.8. The control method was implemented on our robot, and we chose hip joint as the example. The rapidity of the MBPC system is better than the BPC system; however the MBPC system has a larger overshoot and longer transient time. That because the antagonist force of the MBPC system is very small which results in a more flexible character of the joint.

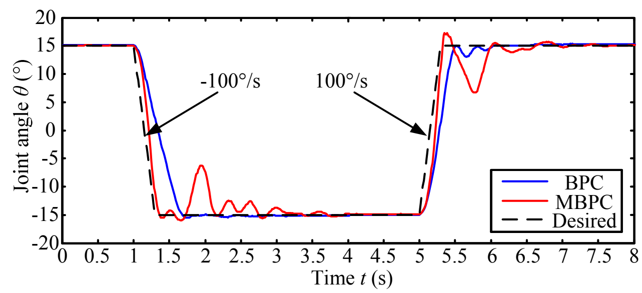

Figure 8. The comparasion of the joint angles' variation for two control method. The blue line presents the results of the basic position control method (BPC), and the red line respresents the results of the model based position control method (MBPC)

■ Accuracy

The steady-state error is another property to evaluate the controller. From (1), we can see that the joint system is a typical second-order system. If we choose the PID controller, the open-loop transfer function of the whole system will contain an integral unit. Thus, for the slope input, the steady-state error is

$$e_{ss}(\infty)=\lim_{s\to 0} sE(s)=\lim_{s\to 0}(s\frac{1}{1+G(s)}\cdot\frac{1}{s^2})=\frac{1}{\lim_{s\to 0} sG(s)}\,. \quad (11)$$

G(s) is the open-loop transfer function with an integral unit. Thus, the $e_{ss}(\infty)$ is constant and equal to the reciprocal value of the system gain, $1/K$. In the same way, the $e_{ss}(\infty)$ for the step input is zero. As shown in Fig.8, the system has an error during slope process, while there is nearly no errors on the step segments.

■ Stiffness

Joint stiffness is a main factor influencing the joint swinging. As (9) and (10) shows, the stiffness is related to the muscles pressures at a fix position. As shown in Fig.9, the pressures for the two control methods were plotted, which were implemented on the hip joint. The joint is swinging from -15° to 15° with a slope 100°/s. The pressures of the steady state are P_1=2.55bar, P_2=4.72bar for the BPC system and P_1=0.69bar, P_2=2.43bar for the MBPC system. Taking the pressures and the structure data into (9) and (10), we can obtain the joint stiffness at the steady state, which are 137Nm/rad for the BPC system, and 69.7Nm/rad for the MBPC system. The variations of the joint stiffness are shown in Fig.9 (d). The joint stiffness for the BPC system is maintaining a higher level than the MBPC system during the entire process. Even during the slope segment, the stiffness of the MBPC system is lower than its normal level. Note that the shadow areas in Fig.9 (a) and (c) present the muscles' function exchanging. That is why there is a large fluctuation around the desired angle for the MBPC system.

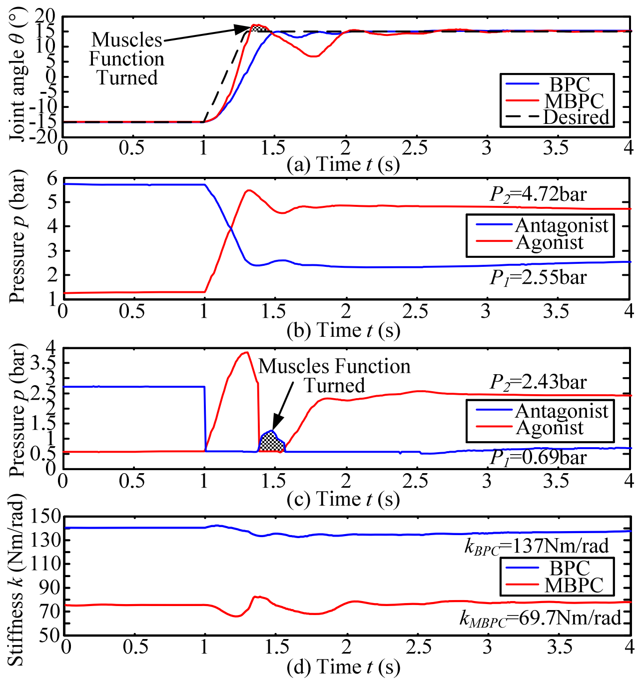

Figure 9. The variation of the muscles pressure for two control method. (a) is the variation of the joint angle. (b) and (c) present the pressure of the BPC system and MBPC system independently. (d) presents the variations of the joint stiffness.

D. *Antagonistic Bionic Joint Control Architecture*

For the legged robot, the rapidity and the accuracy are the main goals of the joint control, meanwhile, it need a higher stiffness at the target position and compliance during the movements. During joint swinging, it is better more flexible to get a fast reflex, and it is better stiffer while reaching the desired angle to hold the position. The flexibility need less antagonist force, and obversely, the accuracy need larger antagonist force.

These two control methods discussed above have their own properties on rapidity, accuracy, and system stiffness. Thus, combining control strategy is proposed as shown in Fig.10. The combining control strategy is the controller we implemented on our robot system. It is a tradeoff between the accuracy and the rapidity. The fundament of the controller is to select the good properties of the BPC and the MBPC. As shown in the diagram, Fig.10, through the comparison of the desired angle and the current angle, it generates a switching signal to choose whether the BPC or the MBPC. When the joint is swinging, the MBPC is operating under a low stiffness, which gives system good compliance and better rapidity. Till the joint reaching the desired angle, the BPC is operating to hold the position of the joint. Within the steady state area, the BPC is chose to obtain a large stiffness which could resist the perturbation and cause a better accuracy.

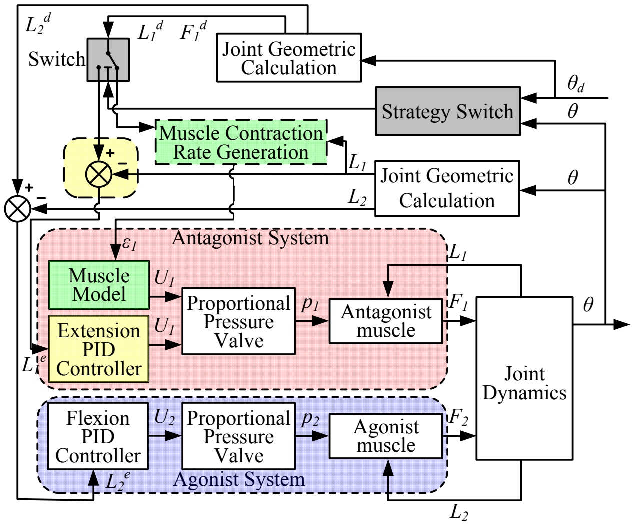

Figure 10. The antagonistic bionic joint control architecture.

IV. Experimental Results

The step test is done by the combining control strategy on the hip joint. The angle were varied from -15° to 15° with a slope 100°/s as shown in Fig.11(a). The joint swinging was nearly not lagging behind, and with a small overshot 3.8°. As we desired the MBPC method was operating during swinging and the BPC method was implemented when the joint within the range of the target angle. The joint exhibits a good rapidity under the MBPC controlling with the very low force of the antagonist, and a well accuracy by the BPC controller. The joint swung from 1s, and only used 0.32s it reached the desired angle, which is just trailed behind 0.02s. Till 1.74s, the variations of the joint angle were within the range of ±5%. From Fig.11(b), we can clearly identify the operation of the BPC and MBPC through the variation of the pressure. The antagonist pressure is low and nearly invariable during MBPC, while, both the pressures are varying under the PID algorithm.

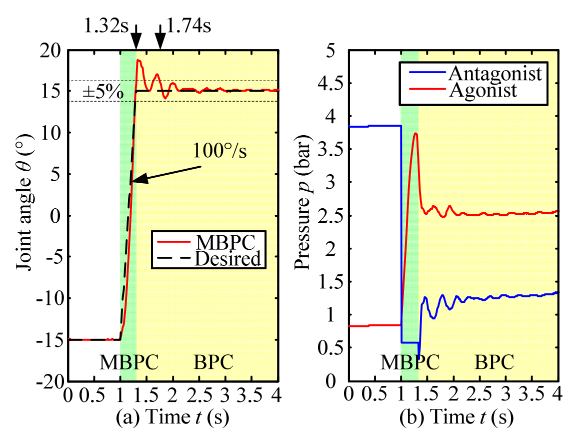

Figure 11. The step test of the antagonistic bionic joint control method. (a) is the variation of the joint angle. (b) presents the pressure of the combining control strategy. The green shadow presents the operating time of the MBPC system. The yellow area is the operating time of the BPC system.

Through (9) and (10), we can calculate the joint stiffness during swinging as shown in Fig.12. The combining controller achieved to turn the joint stiffness under different system status. The stiffness was turned very low when the joint began swinging to obtain the flexibility and the rapidity. It is increasing till the joint reach the desired angle with the maximum 129.26Nm/rad. The large stiffness can improve the system stability and fast reduce the oscillation. Than the BPC method was operating to maintain the joint angle and finally stay at an optimal stiffness 102Nm/rad.

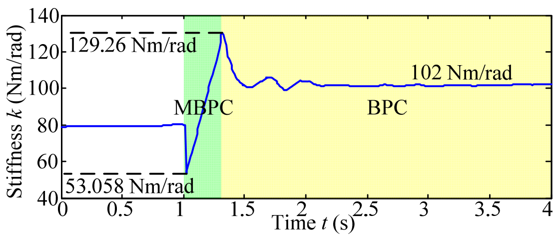

Figure 12. The variation of the joint stiffness under the combining control strategy.

At last, the experiments carried out with the robot, which is aimed at verifying the validity of the system with the herein proposed antagonistic bionic joint controller. The robot was fixed on a falsework as Fig.1 shown and swings the leg in the air. The joints trajectories during running were shown in Fig.13. The aim of this experiment is to test the ability of the joint control algorism to operate robot agilely and accurately. The speed of the legs swinging is 100°/s and the generation of the joints angle are from upper controller as we discussed in previous paper [13, 14]. The results showed that the joint controller could implement the robot's coordinated movements.

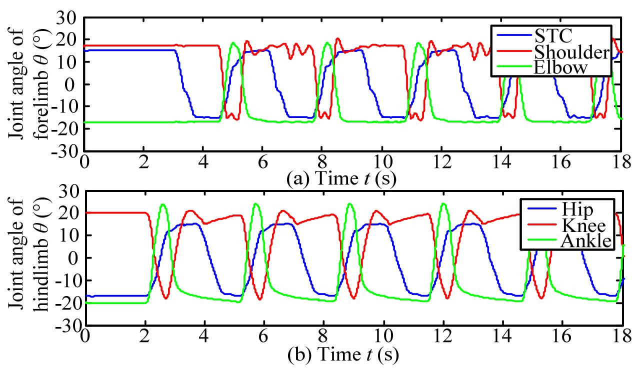

Figure 13. The sequence of the robot's movement cycle.

V. Conclusion

In this paper, a study is performed considering adapting the pneumatic dynamic model and the traditional proportional integral differential control method. The muscle model we proposed here is adjusted from Tondu-Lopez model, which has a higher fitting rate and simpler format. Through the discussion of two joint control methods, it was shown that for the antagonistic bionic joint system a combining control algorism could obtain better performance. A strategy was proposed to make a tradeoff between rapidity and accuracy through combining the basic position control method (BPC) and the model based position control method (MBPC). The idea behind the mathematical formulation of the control algorism is to adjust the stiffness of the pneumatic muscles according to the status of the joint movement. The experiments on our musculoskeletal verified the joint controller could implement robot's coordinated movements agilely and accurately. In the future, we will optimize the joint controller and test the robot running performance.

References

[1] B. Tondu, et al., "Naturally compliant robot-arms actuated by McKibben artificial muscles," in Systems, Man, and Cybernetics, 1994 IEEE International Conference on, pp. 2635-2640 vol. 3.

[2] T. Kerscher, et al., "Evaluation of the Dynamic Model of Fluidic Muscles using Quick-Release," in Biomedical Robotics and Biomechatronics, 2006 The First IEEE/RAS-EMBS International Conference on, pp. 637-642.

[3] I. Mizuuchi, et al., "Development of musculoskeletal humanoid Kotaro," in Robotics and Automation, 2006 IEEE International Conference on, pp. 82-87.

[4] Y. Nakanishi, et al., "Realization of large joint movement while standing by a musculoskeletal humanoid using its spine and legs coordinately," in Intelligent Robots and Systems, 2008 IEEE/RSJ International Conference on, pp. 205-210.

[5] Y. Nakanishi, et al., "Development of musculoskeletal humanoid kenzoh with mechanical compliance changeable tendons by nonlinear spring unit," in Robotics and Biomimetics (ROBIO), 2011 IEEE International Conference on, pp. 2384-2389.

[6] Y. Asano, et al., "Lower thigh design of detailed musculoskeletal humanoid "Kenshiro"," in Intelligent Robots and Systems (IROS), 2012 IEEE/RSJ International Conference on, pp. 4367-4372.

[7] J. C. Albiez, et al., PANTER - prototype for a fast-running quadruped robot with pneumatic muscles. Westminister: Professional Engineering Publishing Ltd, 2003.

[8] K. S. Aschenbeck, et al., "Design of a Quadruped Robot Driven by Air Muscles," in Biomedical Robotics and Biomechatronics, 2006 The First IEEE/RAS-EMBS International Conference on, pp. 875-880.

[9] R. W. Colbrunn, et al., "Design and control of a robotic leg with braided pneumatic actuators," in Intelligent Robots and Systems, 2001 IEEE/RSJ International Conference on, pp. 992-998 vol.2.

[10] B. Vanderborght, et al., "Development of a compliance controller to reduce energy consumption for bipedal robots," Autonomous Robots, vol. 24, pp. 419-434, May 2008.

[11] J. Schroder, et al., "Dynamic pneumatic actuator model for a model-based torque controller," in Computational Intelligence in Robotics and Automation, 2003 IEEE International Symposium on, pp. 342-347 vol.1.

[12] Y. Yamada, et al., "Neural-body coupling for emergent locomotion: A musculoskeletal quadruped robot with spinobulbar model," in Intelligent Robots and Systems (IROS), 2011 IEEE/RSJ International Conference on, pp. 1499-1506.

[13] X. Wang, et al., "Design and development of a cheetah robot under the neural mechanism controlling the leg's muscles," in Intelligent Robots and Systems (IROS), 2012 IEEE/RSJ International Conference on, pp. 2749-2755.

[14] X. Wang, et al., "Bio-Inspired Controller for a Robot Cheetah with a Neural Mechanism Controlling Leg Muscles," Journal of Bionic Engineering, vol. 9, pp. 282-293, Sep 2012.

[15] C. Ching-Ping and B. Hannaford, "Static and dynamic characteristics of McKibben pneumatic artificial muscles," in Robotics and Automation, 1994 IEEE International Conference on, pp. 281-286 vol.1.

[16] V.-M. Tri, et al., "A New Approach to Modeling Hysteresis in a Pneumatic Artificial Muscle Using The Maxwell-Slip Model," Mechatronics, IEEE/ASME Transactions on, vol. 16, pp. 177-186, 2011.

[17] B. Tondu and P. Lopez, "Modeling and control of McKibben artificial muscle robot actuators," Control Systems, IEEE, vol. 20, pp. 15-38, 2000.

[18] B. Tondu, "Modelling of the McKibben artificial muscle: A review," Journal of Intelligent Material Systems and Structures, vol. 23, pp. 225-253, February 1, 2012 2012.